TEMPERATURE-INDUCED STRUCTURAL CHANGES IN EVEN-ODD NYLONS WITH LONG POLYMETHYLENE SEGMENTS

Cristian Olmo[1], Ramon Rota, Juan Carlos Martinez[2], Jordi Puiggalí[1]*, Lourdes Franco[1*]

[1]Departament d'Enginyeria Química, Universitat Politècnica de Catalunya, Av. Diagonal 647, Barcelona E-08028, SPAIN

[2]ALBA Synchrotron Light Facility, Ctra. BP 1413 km. 3,3 08290 Cerdanyola del Vallès, Barcelona, SPAIN (www.albasynchrotron.es)

***Correspondence to*: Jordi Puiggalí (E-mail: Jordi.Puiggali@upc.edu) and Lourdes Franco (E-mail: Lourdes.Franco@upc.edu)**

ABSTRACT

Structural transitions of nylons 8 9 and 12 9 during heating and cooling processes were investigated using calorimetric, spectroscopic and real time X-ray diffraction data. These even-odd nylons had three polymorphic forms related to structures where hydrogen bonds were established in two planar directions. Heating processes showed a first structural transition at low temperature where the two strong reflections related to the packing mode of the low temperature structure (form I) disappeared instead of moving together and merging into a single reflection, as observed for conventional even-even nylons. The high temperature structure corresponded to a typical pseudohexagonal packing (form III) attained after the named Brill transition temperature. Structural transitions were not completely reversible since an intermediate structure (form II) became clearly predominant at room temperature in subsequent cooling processes.

A single spherulitic morphology with negative birefringence and a flat-on edge-on lamellar disposition was obtained when the two studied polyamides crystallized from the melt state. Kinetic analyses indicated that both nylons crystallized according to a single regime and a thermal nucleation. Results also pointed out a secondary nucleation constant for nylon 12 9 higher than that for nylon 8 9, suggesting greater difficulty in crystallizing when the amide content decreased.

Keywords: Polyamides, Brill transition, synchrotron radiation, hydrogen bonds, spherulite, crystallization kinetics.

INTRODUCTION

Nylons, or aliphatic polyamides, are important industrial materials due to their excellent physical properties which include high strength, abrasion resistance, ductility and good stability at high temperatures.[1,2] Recent studies have also demonstrated that several nylons derived from odd units might be interesting for electroactive applications[3]. The geometry and density of hydrogen bonds play a key role in the crystallization process, the crystalline structure and the final properties of nylons.[4] In general, nylons are semicrystalline polymers capable of adopting different crystalline structures depending on the number and parity of methylene groups of their repeat unit. The most conventional structures of nylons are found in even derivatives (i.e. those synthesized from ω-amino acids and those obtained from diamines and dicarboxylic acids). These structures are based on the stack of sheets composed of hydrogen bonded molecular chains.[5-11] The chain folded sheets are held together by weak van der Waals forces and may have different packing modes (e.g. the progressive and alternating shear characteristic of α and β forms, respectively).[4] The corresponding X-ray fiber diffraction patterns of such structures are characterized by the presence of two strong equatorial reflections associated with intrasheet and intersheet spacings and appearing close to 0.440 and 0.380 nm, respectively.

On heating, even and even-even nylons can undergo a transition still not well understood where the two strong reflections in the diffraction patterns are seen to move together and meet, typically at a spacing close to 0.415 nm which defines a pseudohexagonal phase. The temperature at which this phenomenon occurs is the so called Brill transition temperature.[12] For even-even nylons with one or more relatively short alkane segments, this temperature is below the melting point, while for most others the two temperatures are practically coincident.[13] Note that the melting point

increases with the density of hydrogen bonds along the chain, and consequently the structural transition can be observed for nylons with short aliphatic segments.

Brill transition has been widely discussed for nylons having the indicated sheet structure but interpretation is still controversial, especially when other polymorphic forms can be observed. For example, a new pseudohexagonal structure was described for some nylons (e.g. nylon 6[14]) depending on the temperature at which they crystallized from the melt. This phase, which was obtained at high supercoolings, rendered the Brill structure on heating and the typical sheet structure on cooling. In addition, other nylons adopt another pseudohexagonal structure known as *γ-phase*, which is characterized by the establishment of intersheet hydrogen bonds between parallel chains.[15] In the case of nylon 6, the γ structure cannot undergo polymorphic transitions on both heating and cooling runs, and could therefore be distinguished from the above indicated pseudohexagonal form. The hydrogen bonding pattern of this structure is probably different from that found in the γ-phase (i.e. intrasheet hydrogen bonds between antiparallel chains are established) despite the similarity of the packing spacings.

Attention was consequently paid to the hydrogen bonding arrangement during heating and cooling processes. First interpretations assumed a reorganization of hydrogen bonds during heating that gives rise to a network where hydrogen bonds are established along three planar directions that contrasts with the initial one-dimensional hydrogen bonding arrangement.[16,17] This model therefore implies the breakage of some intrasheet hydrogen bonds and the formation of intersheet bonds. The latter can counteract a weakening of the van der Waals interactions between layers as the intersheet spacing increases because of thermal dilatation. Note that the population of hydrogen bonds can be different in the three trigonal directions, and that is why properties (e.g. birefringence) along them may vary. Alternatively, some authors argued from NMR and

FTIR results that hydrogen bonds do not break during heating, and consequently the sheet-like structure remains at high temperatures.[18-22] Basically, the methylene segments started to disorder and the torsional angles of amide–CH_2 bonds changed. In parallel with these structural changes, the hydrogen bonds became gradually weaker.

Different structures with hydrogen bonds established along more than one direction have also been postulated for nylons. Logically, in this case, breakage of intermolecular interactions is not necessary to justify temperature-induced structural changes, which are mainly a consequence of the increasing degrees of freedom of the alkane segments. Formation of a network of intermolecular hydrogen bonds can be justified by: a) Conformational preferences of peculiar residues such as glycine and malonic acid, and b) Optimization of the hydrogen bonding geometry. Specifically, alternate copolymers[23] and oligomers[24] constituted by ω-amino acid and glycine units adopt a similar structure (i.e. with three planar hydrogen bonding directions) to that described for polyglycine II,[25] whereas structures with two hydrogen bonding directions have been postulated for polyamides[26] derived from a diamine and malonic acid. This kind of structure was also deduced from crystallographic analysis of small model compounds.[27]

Nylons having odd diamine or dicarboxylic units (i.e. odd-even or even-odd nylons) cannot form the typical sheet structure when molecular chains have an extended planar zigzag conformation as shown in Figure 1. Nevertheless, X-ray diffraction patterns of solution crystallized samples usually showed the typical strong reflections of conventional nylons (e.g. those appearing at spacings close to 0.440 and 0.380 nm). This feature has been described for both odd-even nylons, such as 5 6,[28,29] 5 10,[30], 9 2,[31,32] 11 10,[33] 11 12,[33] and 13 6,[34] and even-odd nylons like 6 5,[35,36] 12 5,[37] 6 13,[38] 4 7[39] and 6 9.[40,41] Therefore, a new structure based on a molecular chain conformation that causes a slight rotation of consecutive amide groups of the odd diamide unit was

proposed. This structure allows the establishment of strong hydrogen bonding interactions with four neighboring chains when they were conveniently shifted along the chain axis direction.

Accurate analyses of diffraction patterns performed during heating and cooling runs of some representative even-odd nylons having the indicated two-hydrogen bonding structure (named as form I) demonstrated that a pseudohexagonal phase (named as form III) was attained at high temperature. However, a new intermediate structure close to a pseudohexagonal form (named as form II) could also be observed in some cases. Thus, nylons 4 7[39] and 6 9[41] gave predominantly rise to form II when crystallized from the melt state, but a partial transition towards form I could be detected at low temperature (e.g. 80-100 ºC). On the contrary, solution crystallized samples showed a well differentiated behavior on heating. Specifically, nylon 4 7 underwent a complete transition towards form II at a temperature that was again close to 100 ºC (while nylon 6 9 showed only a direct transition from form I to form III). The structural changes from form I to form II seem only to involve a change in the rotation angle between consecutive amide groups of the odd unit and a slight modification in the packing geometry. That is, a breakage of hydrogen bonds is not expected at such low temperatures. In addition, this transition influences on properties and specifically a reversible change on the birefringence spherulite sign has been reported[39, 41].

The different structural behavior of nylons 4 7 and 6 9 on heating is difficult to explain considering their similar crystalline structure at low temperature (i.e. form I). Therefore, a possible influence of the length of the polymethylene segment should be taken into account. Note that both diamine and dicarboxylic units are longer for nylon 6 9. The present work is focused on the study of nylons 8 9 and 12 9, whose diamine unit is slightly or considerably longer than that of nylon 6 9. A second goal of the paper is the

melt crystallization study (i.e. morphology and kinetics) of these polyamides characterized by a peculiar structure different from that of conventional nylons. Although the spherulitic morphology of several even-odd polyamides has previously been studied,[29,39,41,42] no data concerning crystallization kinetics have been reported.

EXPERIMENTAL SECTION

Materials and synthesis

All reagents and solvents were purchased from Sigma-Aldrich and used without purification. Nylons 8 9 and 12 9 were synthesized by interfacial polycondensation of azeloyl dichloride with 1,8-diaminooctane and 1,12-diaminododecane, respectively. Nylon 8 9 was initially synthesized by dropwise addition of approximately 15 mmol of the dichloride dissolved in 75 mL of dry carbon tetrachloride to 75 mL of a stirred aqueous solution containing 15 mmol of 1,8-diaminooctane and 2.4 g of sodium hydroxide. After addition was complete a film was formed at the interface but the final molecular weight was moderate (M_n = 13,000 g/mol). This synthesis was improved according to the method reported for nylon 6,10[43], where an excess of diamine was employed (i.e. ×2.5), the sodium hydroxide was substituted by sodium carbonate and the organic solution was vigorously stirred before addition of the aqueous layer.

This method was slightly modified again for the synthesis of nylon 12 9 due to the water insolubility of the 1,12-diaminododecane. In this case, the diamine was dissolved in a mixture of water/acetone (2:1). A powdered polymer was formed instead of a continuous film and consequently reaction was carried out under stirring for a minimum period of 30 min.

Nylons 8 9 and 12 9 were in both cases recovered by filtration, washed successively with water, ethanol and ethyl ether before drying in a vacuum desiccator at 60 ºC. After that they were purified by precipitation with water of dilute formic acid solutions.

Measurements

Molecular weights were estimated by size exclusion chromatography (GPC) using a liquid chromatograph (Shimadzu, model LC-8A) equipped with an Empower computer program (Waters). A PL HFIP gel column (Polymer Lab) and a refractive index detector (Shimadzu RID-10A) were employed. The number and weight average molecular weights were calculated using polymethyl methacrylate standards.

Infrared absorption spectra were recorded, at a resolution of 4 cm^{-1}, with a Fourier transform FTIR 4100 Jasco spectrometer. A Specac model MKII Golden Gate attenuated total reflection (ATR) with a heated Diamond ATR Top-Plate was used for evaluation of thermal transitions.

^{1}H spectra were recorded on a Bruker AMX-300 spectrometer at 25.0 °C operating at 300.1 MHz. Samples were dissolved in a mixture of deuterated chloroform and trifluoroacetic acid (9:1), and spectra were internally referenced to tetramethylsilane (TMS).

Calorimetric data were recorded by differential scanning calorimetry using a TA instrument Q100 series equipped with a refrigerated cooling system (RCS) operating from -90 ºC to 550 ºC. Experiments were performed under a flow of dry nitrogen with a sample of approximately 5 mg. The instrument was calibrated for temperature and heat of fusion using an indium standard. T_{ZERO} technology required two calibrations, with empty pans and sapphires discs.

Thermal characterization of polymers was carried out following a three run protocol consisting in a heating run (20 ºC/min) of the as-synthesized sample, a cooling run (10 ºC/min) after keeping the sample in the melt for three minutes and a second heating run (20 ºC/min) of the non-isothermally crystallized sample.

Spherulites were grown from homogeneous melt-crystallized thin films produced by melting 1 mg of the polymer on microscope slides. Next, small sections of these films were pressed between two cover slides and inserted in the hot stage. Samples were kept, for 3 minutes, at a temperature 10 degrees higher than the melting point to wipe out sample history effects and then quickly cooled to the selected crystallization temperature. The spherulite growth rate was determined by optical microscopy using a Zeiss Axioscop 40 Pol light polarizing microscope equipped with a Linkam temperature control system configured by a THMS 600 heating and freezing stage connected to an LNP 94 liquid nitrogen cooling system. Micrographs were taken with a Zeiss AxiosCam MRC5 digital camera at appropriate time intervals. A first-order red tint plate was employed to determine the sign of spherulite birefringence under crossed polarizers.

The real-time synchrotron study, at variable temperature, was carried out on beamline BL11-NCD at ALBA (Cerdanyola del Vallés, Barcelona, Spain), by using a wavelength of 0.100 nm and a WAXD LX255-HS detector from Rayonix. Polymer samples were confined between Kapton films and then held on a Linkam hot stage with temperature control within ± 0.1 ºC. WAXD profiles were acquired during heating and cooling runs in time frames of 20 s and rates of 10 ºC/min. The WAXD diffraction patterns were calibrated by means of a geometrical calibration process of a well-known sample (standard Cr_2O_3). The diffraction profiles were normalized to the beam intensity and corrected considering the empty sample background.

RESULTS AND DISCUSSION

Chemical characterization

The chemical constitution was checked by infrared and ^{1}H NMR spectroscopies and both, molecular weight and polydispersity index were estimated by GPC. Nylon 8 9 was obtained with a yield of 60%, polydispersity index of 2.5 and number average molecular

weight of 21,000. The corresponding values for nylon 12 9 were 70%, 2.1 and 15,000, respectively.

Infrared spectra of the two studied nylons showed all the characteristic absorption bands of amide and methylene groups at: ≈ 3302 cm^{-1} (Amide A, N-H stretching), ≈3079 cm^{-1} (Amide B, overtone of amide II), 2922-2917 and 2850 cm^{-1} (asymmetric and symmetric CH-stretching bands), ≈ 1633 cm^{-1} (Amide I, C=O stretching), ≈ 1545 cm^{-1} (Amide II, C-N stretching and CO-N-H bending), ≈ 940 cm^{-1} (Amide IV, C-CO stretch), ≈ 721 cm^{-1} (CH_2 waging), ≈ 690 cm^{-1} (Amide V, N-H out of plane bending) and ≈ 580 cm^{-1} (Amide VI, C=O out of plane bending).

^{1}H NMR spectra were characterized by peaks at: 3.56 ppm (NHCH_2, broad, 4H), 2.65 ppm (COCH_2, triplet, 4H), 1.76 ppm (NHCH_2CH_2, broad, 4H), 1.71 (COCH$_2$CH_2, broad, 4H) and 1.41 ppm (-$(CH_2)_4$- + -$(CH_2)_5$-, broad, 16H) for nylon 8 9 and 3.51 ppm (NHCH_2, broad, 4H), 2.65 ppm (COCH_2, triplet, 4H), 1.73 ppm (NHCH_2CH_2, broad, 4H), 1.71 (COCH$_2$CH_2, broad, 4H) and 1.35 ppm (-$(CH_2)_8$- + -$(CH_2)_5$-, broad, 24H) for nylon 12 9.

Thermal properties

Figure 2 shows a sequence of three scans performed with the as-synthesized nylons 8 9 and 12 9 samples. As it was expected, the melting point of nylon 8 9 (T_m = 203 ºC) is higher than that of nylon 12 9 (T_m = 184 ºC) because its ~~dicarboxylic~~ diamine segment is shorter. Also, these temperatures were similar to those determined for other even-odd nylons with the same methylene content as nylons 6 11[44] (T_m = 212 ºC) and 10 11[44] (T_m = 190 ºC). In both cases, the glass transition is clearly visible in the first heating run and appears at very close temperatures (52 ºC for nylon 8 9 and 51 ºC for nylon 12 9). In any case, the solution crystallized samples had a significant amorphous character.

The first heating run of nylon 8 9 presents a defined endothermic peak at 203 ºC and a wide exothermic interval from 90 ºC to 175 ºC, which is indicative of the occurrence of a significant recrystallization process. Note the low melting enthalpy compared with that detected for the melt crystallized sample (i.e. 57 with respect to 79 J/g). The cooling run revealed a narrow exothermic crystallization peak at 178 ºC and a broad exothermal process at lower temperatures, which could be associated to a secondary crystallization or even to a structural transition (see the arrow pointing out a small peak close to 125 ºC). The subsequent heating run showed a complex fusion where the main peak at 203 ºC is preceded by two smaller peaks (180 ºC and 191 ºC). The intermediate temperature endothermic peak can be a consequence of the melting of thin lamellar crystals having the high temperature structure (i.e. form III), the lowest temperature peak can be related to defective lamellar crystals having a crystalline structure different from form III (e.g. form II), and finally the highest temperature peak is attributed to the melting of recrystallized crystals during the heating process.

The melting behaviour is slightly different for nylon 12 9. In this case, the first run presents a main and broad melting peak at 184 ºC and two small and broad peaks at 130 ºC and 160 ºC. The last temperature is very low for a melting process and probably both endotherms should be related to structural transitions (e.g. from form I to form II and from form II to form III). Note that nylon 8 9 showed also the endotherm at 180 ºC whereas the previous one could not be detected due to the significant exothermic process that took place at the low temperature range. It should be pointed out that an exothermic process during the first heating run of nylon 12 9 cannot be completely discarded due to the initial high amorphous content (revealed by the clear glass transition) and a compensation effect caused by the indicated endothermic processes. The trace of the cooling run is similar than that observed for nylon 8 9 with a narrow

peak at 171 ºC and a broad exothermic peak indicative of a secondary crystallization. It should be again pointed out a small exothermic peak (see arrow) that could be related with a polymorphic transition. The third run is similar to the first one thought the main endothermic peak appears at a higher temperature (i.e. 189 ºC). Melting enthalpy is clearly higher than determined in the first heating run and agree with the crystallization enthalpy of the second run. For this reason, the second heating run does not reveal any exothermic process in the 100-175 ºC temperature interval and on the contrary, small endotherms are clearly visible despite they may involve transitions of very minor phases as then will be discussed.

The difference between the melting temperature (T_m) and the crystallization temperature (T_c) (i.e. ΔT) points out an easier crystallization process for nylon 12 9 as a consequence of its lower molecular weight (i.e. values of 25 ºC and 13 ºC were determined for nylons 8 9 and 12 9, respectively).

Equilibrium melting temperatures of nylons 8 9 and 12 9

Figure 3a illustrates the melting behaviour of nylon 12 9 samples isothermally crystallized at different temperatures in the 175 ºC - 185 ºC range. In this case, low temperature endotherms (i.e. those appearing at 130 and 160 ºC) could logically not be detected and the high temperature peak appeared clearly splitted when the sample was crystallized at the lowest temperature. The low temperature peak seems to be associated with thinner crystals and gradually shifted to higher temperatures and increased on intensity when the crystallization temperature was raised. The high temperature peak, which appears around 190 ºC, is related with the thicker crystals formed during the heating scan as a consequence of a lamellar reorganization and consequently was always observed at the same temperature. Logically, the reorganization process was more significant when the sample was crystallized at the lowest temperature, being in

this case more intense the high temperature peak and greater the temperature difference between the two endotherms. A similar behavior was observed for nylon 8 9, being the above indicated peaks at 191 and 204 ºC related to the reorganization process.

A linear Hoffmann-Weeks relation[45] has been widely accepted to estimate equilibrium melting point (T_m^o), defined as the melting temperature of infinitely thick crystals, which is determined by extrapolation of T_m versus T_c to $T_m = T_c$. Equilibrium melting temperatures of 202 ºC and 219 ºC were graphically deduced for nylons 12 9 and 8 9, respectively (Figure 3b).

Wide angle X-ray diffraction analyses of nylon 8 9 polymorphic transitions during heating and cooling processes

Figure 4a shows a three-dimensional representation of the evolution of the WAXD profile of the as-synthesized nylon 8 9 during a heating process performed at 10 ºC/min from room temperature to fusion, whereas one-dimension profiles taken at some representative temperatures are given in Figure 4b.

At the beginning of the experiment, nylon 8 9 presented two very intense reflections corresponding to spacings of 0.442 and 0.370 nm, which are characteristic of the structure with two hydrogen-bonding directions (form I). Also, another two reflections, at 0.430 and 0.395 nm (Form II), with very low intensity, can be glimpsed at room temperature. Note that these spacings are clearly different from those found close to 0.415 nm in nylons having a pseudohexagonal γ structure with a single hydrogen bonding direction. As temperature increases the intensity of the former signals slightly decreased at the beginning (i.e. up to 95 ºC) and then (i.e. between 95 and 120 ºC) practically disappeared. The spacing of the 0.370 reflection gradually increased during heating (i.e. up to 0.384 nm) while 0.442 reflection decreased only up to 0.440 nm. At the same time the 0.430 and 0.395 nm diffraction signals increased their intensity and

move together with increasing the temperature, meeting at a single spacing of 0.428 nm just before the melting point. The existence of a single peak suggests a typical Brill transition where a pseudohexagonal packing (form III) is favoured at a temperature slightly lower than the melting point.

The intensity of signals at 0.430 and 0.395 nm became more intense from 95 ºC to 150 ºC, temperature at which the conversion from form II to form III began. Beyond 150 ºC the behavior of the signals was different, the intensity of the signal at 0.430 nm remained practically constant, whereas the signal at 0.405 nm (initially at 0.395 nm) became weaker and moved gradually to a higher spacing up to reach the 0.428 nm value.

In the last stages of the heating process, the intensity of the Bragg reflections began to decrease until leading to an amorphous asymmetric halo characteristic of the melt state. The evolution of the different spacings with the temperature is graphically represented in Figure 4c where the occurrence of different transitions is also highlighted.

The observed polymorphic transitions were not completely reversible in a subsequent cooling run (10 ºC/min) up to room temperature. The 3D WAXD profiles given in Figure 5a show that nylon 8 9 first crystallized in the high temperature form III (i.e. a single spacing at 0.428 nm was only observed). Around 160 ºC a weak signal at 0.420 nm, characteristic of form II, started to appear while the intensity of the high spacing reflection clearly decreased. When temperature was around 120 °C the transition from form III to form II was finished, being clearly visible two strong signals at 0.428 and 0.415 nm. The spacing and intensity of the first reflection remained practically constant whereas a decrease was detected for the second one suggesting an anisotropy for thermal contraction. In fact, at room temperature a spacing of 0.405 nm was determined. Around 65 ºC the diffraction pattern showed the apparition of another two very low

intensity signals at 0.443 nm and 0.376 nm that are related with form I. The evolution of the different spacings and the occurrence of the different structural transitions are given in Figure 5b. We can conclude that at room temperature both structures coexist, being form II the predominant one in disagreement with the room temperature pattern of the as-synthesized sample.

For the sake of completeness, Figure 6 shows representative X-ray diffraction profiles and patterns taken at selected temperatures during heating and cooling runs. The difference in the diffraction patterns of the sample taken at 25 °C before heating and after being crystallized from the melt state is therefore highlighted. Thus, in both cases four rings associated to forms I and II can be detected, but the ratio between them changed drastically (i.e. forms I and II are predominant in the initial sample and the melt crystallized one, respectively). Note also that reflections of both structures have a similar intensity in the diffraction pattern taken at 95 ºC during the heating process.

In summary, it can be concluded that nylon 8 9 has two different crystalline structures at room temperature depending on the thermal treatment of the sample. These structures are probably related to molecular arrangements where hydrogen bonds are established along two directions since transitions involving the breakage of intermolecular hydrogen bonds seem difficult to be favoured at temperatures so low as 75 ºC-95 ºC. In any case, transitions from form I to form II and from form II to form III took place in wide temperature intervals that could be related to the low and broad peaks observed in the DSC scans.

Wide angle X-ray diffraction analyses of nylon 12 9 polymorphic transitions during heating and cooling processes

The evolution of the X-ray diffraction profiles of the as-synthesized sample during heating at 10 ºC/min (Figure 7a) is highly similar to the above explained evolution of

nylon 8 9. Thus, four reflections can be clearly observed in the initial pattern, two more intense at 0.446 and 0.382 nm that are related to form I and two other less intensity reflections at 0.430 and 0.400 nm that are related to form II. However, note that the initial proportion of form II is clearly higher for nylon 12 9 than for nylon 8 9. Around 120 ºC the intensity of the former pair of signals decrease significantly whereas the latter pair of signals start to increase on intensity, suggesting the occurrence of a form I to form II structural transition. This is in clear agreement with the endothermic peak observed in the DSC heating scan. The peak at 0.400 nm shifted progressively to a larger spacing until reached the peak at 0.430 nm at a temperature of 175 ºC. A typical pseudohexagonal arrangement (form III) is completely attained before to start the melting process.

Figure 7b shows the evolution of the spacing of the different signals during the heating process. One dimensional WAXD profiles and diffraction patterns taken at selected temperatures are given in Figure 8 to show more clearly the structural transitions. Hence, both structures have a similar relevance in the profile taken at 125 ºC. A single peak, related to form III was observed at 175 ºC, just before melting where an amorphous halo was detected. It should be pointed out the similar evolution of reflections for nylons 8 9 and 12 9 that agrees with that previously reported for nylon 4 7[39] and differs to that observed for nylon 6 9[41] where only a form I to form III transition was detected on heating. In this way, the observed polymorphism does not seem to be related to the length of the polymethylene segment but on the contrary seems to be dependent on the presence in the initial sample of reminiscent crystals having the form II structure as it is the case of nylons 4 7,[39] 8 9 and 12 9 but not for nylon 6 9.[41]

When the polymer is cooled from the melt (Figure 9) crystallizes into form III as deduced from the single reflection at 0.430 nm. Nevertheless, this reflection became

immediately splitted in the two characteristic reflections of form II (i.e. 0.428 nm and 0.420-0.405 nm). Note that the intensity of the high spacing reflection clearly decreases in the 150 ºC -125 ºC temperature interval while the reflection at 0.420 nm increases on intensity and moved towards a spacing of 0.405 nm. The transition from form III to form II mainly took place in this temperature range, a feature that is agreement with the broad and exothermic peak detected in the corresponding DSC scan. At the end of the cooling process the diffraction pattern consists in two rings at 0.405 and 0.421 nm but also very weak signals associated to form I can be guessed.

Results also indicated that different ratios between form I and form II could be achieved at room temperature depending on the crystallization process (i.e. from solution or from the melt). Furthermore, thermal treatment also influenced on this ratio as shown in the patterns of Figure 10. Thus, a high ratio of form I was still observed when the as-synthesized sample was cooled after being heated at a temperature of 150 ºC. Namely, at a temperature where the transition to form II was practically completed. On the contrary form II became predominant when the sample was heated up to 175 ºC (i.e. before fusion). Nevertheless, a small proportion of form I could still be observed at room temperature and specifically the corresponding signals were stronger than those guessed for melt crystallized samples. It should be pointed out that some reminiscence of form I crystals should still occur at 175 ºC in such a way that could act as nuclei for the development of such structure on the subsequent cooling process.

Temperature dependence of infrared amide A band

Crystalline transitions were also evaluated through FTIR spectra taken during heating and cooling processes. In particular, temperature dependence of amide A band was studied for nylon 8 9 since this polymer gave the greater ratio of form I during cooling (i.e. had the greater reversibility). The amide A band (NH stretching mode) is highly

sensitive to the hydrogen bond geometry and consequently may give additional information concerning structural transitions induced by temperature changes.

Figure 11 shows the evolution of the amide A band from room temperature to the melting temperature for the as-synthesized sample. Three different regions can be distinguished in the plot: Firstly the wavenumber remained practically constant (3295 cm^{-1}) up to a temperature close to 75 ºC which is related to the beginning of a significant recrystallization process (DSC data) and the structural transformation from form I to form II (synchrotron data), secondly a region where the wavenumber gradually increased (i.e. from 3295 to 3308 cm^{-1}) as a consequence of the decrease on the hydrogen bonding strength caused by the development of form II and its higher sensitivity to the thermal expansion, and finally a last region at temperatures higher than 175 ºC where the wavenumber remains again constant (3308 cm^{-1}) and that corresponded to the development of form III (synchrotron data).

When the sample was cooled from 200 ºC to room temperature a decrease in the amide A band frequency was observed in the temperature range between 190 ºC and 110 ºC while a constant value was again detected at higher and lower temperatures (Figure 11). These temperature limits are in agreement with the development of form II from form III (190 ºC) and form I from form II (110 ºC, although this temperature was slightly higher than determined from DSC and synchrotron experiments). Logically the contraction of the cell during the cooling process gave rise to strong hydrogen bonds as consequence of the continuous decrease on the intermolecular distances. The behavior observed in the cooling run was reproduced in a subsequent heating run indicating the reversibility of all the observed transitions. Note also that great differences were found between the first and the second heating run since the predominant starting structure was different in each case (form I and form II).

A crucial factor to consider is that it was not possible to completely melt the sample in these experiments because the temperature controller of the ATR just could reach a maximum temperature of 200 ºC (i.e. slightly lower than the melting temperature of nylon 8 9). Therefore, it was also interesting to evaluate the cooling run of a sample that was previously melted externally on a hotplate. Figure 11 shows a different behavior since the transition to form I took place at a lower temperature (i.e. 90 ºC) that was in this case in full agreement with DSC and X-ray diffraction observations. The different behavior between the two cooling runs can be interpreted as a consequence of a higher difficulty to undertake the transition when residual form I crystals were completely melted, namely when a potential nucleation effect was prevented. Note also that in this case the wavenumber of the Amide A band decreased up to 3286 cm^{-1}, a value that was significantly lower than that observed for the as-synthesized sample (3295 cm^{-1}). This difference is consequence of the predominant crystalline structure that is achieved at room temperature and indicates a better hydrogen bonding geometry for form II with respect to form I.

Spherulitic morphologies

Until now the only studies published in literature on morphology of melt crystallized spherulites of even-odd polyamides derived from azelaic acid are those concerning to nylons 4 9[42] and 6 9[41]. Spherulites of both nylons showed a great diversity of morphologies in function of the crystallization temperature. Nevertheless peculiar and common trends could be detected.

Nylon 4 9 showed the formation in a narrow temperature range of mixed spherulites comprised of a low positively birefringent part and a higher negatively birefringent area. In fact, morphologies were rather complex and ranged from aggregates to not well understood flecked or mottled crystals. Furthermore, some of these spherulites

experienced a change on the birefringence sign during heating/cooling treatments. These preliminary observations were not interpreted from a structural point of view but suggested the occurrence of a reversible polymorphic transition that affected the birefringence sign. Logically, typical justifications given for conventional nylons with a single hydrogen bonding direction cannot be applied.[46,47] Note that a reversible change from a structure with hydrogen bonds aligned with the radial direction (positive birefringence) to a structure with tangential direction alignment (negative birefringence) implies a sheet reorganization that is not possible without producing a melting of the initial spherulite.

Crystallization of nylon 6 9 could also give rise to both, positive and negative spherulites depending on the crystallization temperature[41]. A reversible change in the sign of birefringence was again observed for spherulites developed in a very narrow temperature interval that ranged between 232 ºC and 225 ºC. These spherulites were characterized by a very low birefringence and a flat-on lamellar disposition that allowed detecting small changes derived from a modification on the packing mode. Interestingly, the change on optical properties took place in the low temperature range where a transition from form I to form II was confirmed by synchrotron radiation experiments.

Crystallization experiments performed with nylons 8 9 and 12 9 were limited due to their high nucleation and fast crystal growth. Therefore, isothermal measurements could only be performed in a very narrow temperature range. The observation of the crystallization process under the polarizing optical microscope visually confirmed a thermal nucleation process because new nuclei were emerging over time before impinging upon each other (Figure 12, a-b-c).

Isothermal crystallization of nylon 8 9 from the melt rendered small spherulites with some axialite reminiscences over the studied narrow temperature range. Nylon 12 9 crystallized also from the melt giving rise to spherulites (Figure 12-d) with a fairly defined Maltese cross and a trend to a ringed texture. Regarding to the birefringence sign it did not change, being negative for both nylons at any temperature assayed. It should be emphasized that a flat-edge lamellar disposition was always observed, being unfeasible to detect a birefringence change when small variations on the two-hydrogen bonding scheme took place (i.e. from form II to form I).

Using optical microscopy we measured the growth of individual spherulites as a function of time at different crystallization temperatures. Once they have nucleated, they grew, each with a radius increasing linearly with time (figure 13a) up to impingement. The spherulite growth was studied in the range where spherulites with adequate dimensions formed, from 195 to 203 ºC and from 175 to 185 ºC for nylons 8 9 and 12 9, respectively. The high nucleation density hindered to observe the growth at lower temperatures.

Both nylons showed an exponential dependence of the growth rate with decreasing temperatures but the exact temperature at which maximum rate was attained could not be determined. The measured radial growth rates, G, varied from 0.002 μm/s at 203 ºC to 0.02 μm/s at 195 ºC for nylon 8 9 and from 0.007 μm/s at 185 ºC to 0.10 μm/s at 175 ºC for nylon 12 9. Higher values were always determined for nylon 12 9 (Figure 13b) as presumable from its lower molecular weight.

The radial growth rate, G, of polymer crystals can be described by the Lauritzen and Hoffman equation[48] which is formulated as:

$$G = G_0 \exp\left[-U^*/(R(T_c - T_\infty))\right] \exp\left[-K_g/(T_c(\Delta T)f)\right] \qquad (1)$$

where G_0 is a constant pre-exponential factor, U^* represents the activation energy characteristic of the transport of the crystallizing segments across the liquid-crystal surface, T_∞ is the temperature below which such motion ceases, T_c is the crystallization temperature, R is the gas constant, K_g is the secondary nucleation constant, ΔT is the degree of supercooling measured as T_m-T_0, and f is a correction factor accounting for the variation in the bulk melting enthalpy per unit volume with temperature ($f = 2T_c/(T_m^0 + T_c)$).

The values of U^* and T_∞ hardly affect the temperature dependence of the radial growth rate when isothermal experiments are carried out at temperatures far above the glass transition temperature. Thus, standard values reported by and Suzuki and Kovacs[49] (U^*= 1500 cal/mol and $T_\infty = T_g$-30 K) were used in the calculation.

The rearrangement of the equation 1 in a logarithmic form let to obtain the K_g from the slope of the linear plot of ln $G + U^*/R(T_c-T_\infty)$ versus $1/(T_c(\Delta T)f)$ (shown for nylon 12 9 in Figure 13c).

Secondary nucleation constants of 0.53 x 10^5 K^2 and 0.92 x 10^5 K^2 were determined from nylon 8 9 and 12 9, respectively. The values indicate a greater difficulty for crystallization as the length of methylene chain increases.

CONCLUSIONS

The room temperature structure of as-synthesized samples of nylons 8 9 and 12 9 is characterized by a peculiar arrangement (form I) where hydrogen bonds are established along two planar directions. This structure is characterized by strong X-ray diffraction reflections at spacings close to 0.446-0.442 and 0.382-0.370 nm. The typical behavior of conventional even-even nylons was not observed on heating since an intermediate structure with X-ray diffraction spacings close to 0.430 and 0.400-0.395 nm was developed before to meet in a single reflection above the Brill transition temperature.

Previous works indicated that similar transitions could be found for nylon 4 7 but not for nylon 6 9. In this way, the length of the polymethylene segments does not seem to play a key role in the thermally induced polymorphism of even-odd nylons. The presence in the as-synthesized sample of reminiscent crystals having the intermediate form II structure could probably favour the occurrence of the low temperature transition.

On cooling, form I and form II structures could be detected although the form I was clearly minority. Nevertheless, the ratio of form I increased when the sample was not completely melted in the previous heating run as a consequence of the presence of reminiscent nuclei having this structure.

Both polymers crystallized from the melt as negative birefringent spherulites, following a single crystallization regime and a thermal nucleation process. The increase of the length of the polymethylene segment hinders the crystallization process as reflected by the higher secondary nucleation constant of nylon 12 9.

Acknowledgements. Authors are in debt to supports from MECD and FEDER (MAT2015-69547-R) and the Generalitat de Catalunya (2014SGR188). Diffraction experiments were performed at NCD beamline at ALBA Synchrotron with the collaboration of ALBA staff.

REFERENCES

1. K. Marchildon, *Macromol. React. Eng.* **2011**, *5*, 22-54.
2. C. Bennett, E. Kaya, A.M. Sikes, W. L. Jarret, L.J. Mathias, *J. Polym. Sci. Part. A: Polym. Chem* **2009**, *47*, 4409-4419.
3. S. Liu, Z. Cui, P. Fu, M. Liu, L. Zhang, Z. Li, Q. Zhao, *J. Polym. Sci., Polym. Phys.* **2014**, *52*, 1094-1099
4. A. Xenopoulos, ES. Clark, In Nylon Plastics Handbook; Kohan MI Ed.; Hanser Publishers: Munich, Vienna and New York, **1995**; Chapter 5, pp108-137
5. C. W. Bunn, E. V. Garcner, *Proc R Soc London Ser A* **1947**, *189*, 39-68
6. N.A. Jones, E.D.T Atkins, M.J. Hill, S. J. Cooper, L. Franco, *Macromolecules* **1996**, *29*, 6011-6018
7. M.J. Hill, E.D.T Atkins, *Macromolecules* **1995**, *28*, 604-668.
8. N.A. Jones, E.D.T Atkins, M.J. Hill, S. J. Cooper, L. Franco, *Polymer* **1997**, 38, 2689-2699.
9. L. Franco, J. Puiggali, *J. Polym. Sci., Part B: Polym. Phys.* **1995**, *33*, 2065-2073.
10. N.A. Jones, E.D.T Atkins, M.J. Hill, S. J. Cooper, L. Franco, *Macromolecules* **1997**, *30*, 3569-3578
11. D.E. Holmes, C.W. Bunn, D. Smith, *J. Polym. Sci. Part A, General Papers* **1955**, *17*, 159-177.
12. R. Brill, *Makromol Chem* **1956**, *18*, 294-309.
13. N.A. Jones, E.D.T. Atkins, M.J. Hill, *Macromolecules* **2000**, *33*, 2642-2650.
14. C. Ramesh, E.B. Gowd, *Macromolecules* **2001**, *34*, 3308-3313.
15. Y. Kinoshita, *Makromol Chem* **1959**, *33*, 1-20.
16. R. Brill, *J. Prakt. Chem.* **1942**, *161*, 49-64.
17. S.J. Cooper, E.D.T. Atkins, M.J. Hill, *Macromolecules* **1998**, *31*, 8947-8956.

18. H. Miura, K.H. Gardner, *Macromolecules* **1988**, *21*, 1543-1544.

19. J. Hirschinger, H. Miura, K.H. Gardner, A.D. English, *Macromolecules* **1990**, *23*, 2153-2169.

20. J.J. Wendolowski, K.H. Gardner, J. Hirschinger, H. Miura, A.D. English, *Science* **1990**, *247*, 431-436.

21. Y. Yoshioka, K. Tashiro, C. *Polymer* **2003**, *44*, 6407-6417.

22. K. Tashiro, Y. Yoshioka, *Polymer* **2004**, *45*, 4337-4348.

23. J. Bella, J. Puiggalí, J.A. Subirana, *Polymer* **1994**, *35* , 1291-1297.

24. J. Tormo, J. Puiggalí, J. Vives, I. Fita, J. Lloveras, J. Bella, J. Aymamí, J.A. Subirana, *Biopolymers* **1992**, *32*, 643-648.

25. F.H.C. Crick, A. Rich, *Nature* **1955**, *176*, 780-781.

26. J. Puiggalí, J.E. Aceituno, E. Navarro, J.L. Campos, J.A. Subirana, J.A. *Macromolecules* **1996**, *29*, 8170-8179.

27. V. Tereshko, E. Navarro, J. Puiggalí, J.A. Subirana, *Macromolecules* **1993**, *26,* 7024-7028.

28. J. Puiggalí, L. Franco, A. Alemán, J.A. Subirana, *Macromolecules* **1998**, *31*, 8540-8548.

29. L. Morales-Gámez, A. Ricart, L. Franco, J. Puiggalí, *Eur. Polym. J.* **2010**, *46*, 2063-2077.

30. P. Villaseñor, L. Franco, J.A. Subirana, J. Puiggalí, *J. Polym. Sci. Part B, Polym Phys* **1999**, *37*, 2383-2395.

31. L. Franco, J.A. Subirana, J. Puiggalí, *Macromolecules* **1998**, *31*, 3912-3924.

32. T. Nakagawa, K. Nozaki, S. Maeda, T. Yamamoto, *Polymer* **2015**, *57*, 99-104.

33. X. Cui, D. Yan, *European Polym. J.* **2005**, *41*, 863-870.

34. S. Samanta, J. He, J. Lattimer, C. Ulven, M. Sibi, J. Bahr, B.J. Chisholm, *Polymer* **2013**, *54*, 1141-1149.

35. E. Navarro, J. Franco, J.A. Subirana, J. Puiggalí, *Macromolecules* **1995**, *28*, 8742-8750.

36. L. Morales-Gámez, D. Soto, L. Franco, J. Puiggalí, *Polymer* **2010**, *51*, 5788-5798.

37. E. Navarro, J.A. Subirana, J. Puiggalí, *Polymer* **1997**, *38*, 3429-3432.

38. X. Cui, D. Yan, C. Xiao, *e-polymers* **2004**, 068.

39. L. Morales-Gámez, M.T. Casas, L. Franco, J. Puiggalí, *European Polym. J*. **2013**, *49*, 1354-1364.

40. L. Franco, S.J. Cooper, E.D.T Atkins, S.J. Hill, N.A. Jones, *Macromolecules* **1998**, *36*, 1153-116

41. S. Murase, M.T Casas, J.C. Martínez, F. Estrany, L. Franco, J. Puiggalí, *Polyme*r **2015**, *76*, 34-45.

42. J.H. Magill, *J. Polym. Sci.: Part A-2* **1969**, *7*, 123-142.

43. T.I. Bieber, *Journal of Chemical Education* **1979**, *56*, 409-410.

44. X. Cui, Z. Liu, D. Yan, *European Polymer Journal* **2004**, *40*, 1111-1118.

45. J.D. Hoffman, J.J. Weeks, *J.Res. Nat. Bur. Stand.* **1962**, *66A*, 13-28.

46. A.J. Lovinger, *J. Appl. Phys.* **1978**, *94*, 5003-5013.

47. A. J. Lovinger, *J. Appl. Phys.* **1978**, *49*, 5014-5028.

48. J.I. Lauritzen, J.D. Hoffman, *J. Appl. Phys.* **1973***, 44*, 4340-4352.

49. T. Suzuki, A.J. Kovacs, *Polym. J. 1970, 1*, 82-100.

FIGURE CAPTIONS

Figure 1. Scheme comparing the hydrogen bonding geometry that could be stablished between nylon 8 8 (a) and nylon 8 9 (b) chains having an all trans conformation.

Figure 2. From down to up, calorimetric scans of the heating run of the as-synthesized sample, the cooling run from the melt state and the subsequent heating run of nylon 8 9 (a) and nylon 12 9 (b). Arrows indicate small endothermic and exothermic peaks.

Figure 3. a) DSC heating runs of nylon 12 9 samples after being crystallized from the melt at (from down to up) 176 ºC, 178 ºC, 180 ºC, 181 ºC and 182 ºC. Evolution of main peaks is indicated by the dashed arrows. b) Hoffman-Weeks plot of temperatures corresponding to the melting peak versus crystallization temperature for nylon 8 9 (squares) and nylon 12 9 (triangles). Equilibrium melting temperatures are indicated for both nylons at the intersection point with the T_m=T_c line.

Figure 4. a) Three dimensional representation of WAXD profiles of nylon 8 9, during heating (10 ºC/min) from room temperature to fusion. b) One-dimensional WAXD profiles of nylon 8 9 during heating at selected temperatures. Dashed and dotted lines represent the evolution of the main reflections of form I and form II, respectively. c) Evolution of the main reflections found in the diffraction pattern of nylon 8 9 during the heating process. Full and empty symbols indicate well-defined and intuited reflections, respectively. The temperatures at which structural transitions occur are indicated with vertical lines.

Figure 5. a) Three-dimensional representation of WAXD profiles of nylon 8 9 during cooling (10 ºC/min) from the melt state to room temperature. b) Changes on the spacing of the main reflections of nylon 8 9 during the cooling process. Full and empty symbols indicate well-defined and intuited reflections, respectively.

Figure 6. One-dimensional WAXD profiles of nylon 8 9 taken at selected temperatures during the heating scan (bottom of the graph) and the cooling scan (top of the graph). Dashed and dotted lines represent the evolution of the main reflections of form I and form II, respectively. Diffraction patterns corresponding to some characteristic temperatures are also included.

Figure 7. a) Three dimensional representation of WAXD profiles of nylon 12 9 during heating (10 ºC/min) from room temperature to fusion. b) Evolution of the main reflections found in the diffraction pattern of nylon 12 9 during the heating process. Full and empty symbols indicate well-defined and intuited reflections, respectively. The temperatures at which structural transitions occur are indicated with vertical lines.

Figure 8. One-dimensional WAXD profiles of nylon 12 9 taken at selected temperatures during the heating scan. Dashed and dotted lines represent the evolution of the main reflections of form I and form II, respectively. Diffraction patterns corresponding to some characteristic temperatures are also included.

Figure 9. a) Three-dimensional representation of WAXD profiles of nylon 12 9 during cooling (10 ºC/min) from the melt state to room temperature. b) Changes on the spacing of the main reflections of nylon 12 9 during the cooling process. Full and empty symbols indicate well-defined and intuited reflections, respectively.

Figure 10. X-Ray diffraction patterns of nylon 12 9 at room temperature: a) Sample cooled from the melt state, b) Sample cooled from a partially melted state (i.e. from 175 ºC) and c) Sample cooled after being heated to 150 ºC (i.e. previous to fusion and before disappearance of form I).

Figure 11. Variation of the wavenumber corresponding to the amide A absorption band of nylon 8 9 during a first heating run (full circles), the subsequent cooling (empty

circles) and heating (full triangles) runs and finally a cooling run from an externally melted sample (empty triangles).

Figure 12. Polarized optical micrographs of samples isothermally crystallized at the indicated temperatures and crystallization times: (a) Nylon 8 9 at 200 ºC, 540 seconds; (b) Nylon 8 9 at 200 ºC, 1260 seconds (c) Nylon 8 9 at 200 ºC, 2625 seconds and (d) Nylon 12 9 at 180 ºC, 1850 seconds. A colour micrograph taken with a red tint plate is given in the inset of d) in order to observe the sign of birefringence. All micrographs were taken at the same magnification.

Figure 13. a) Plots of the radius of nylon 12 9 spherulites versus crystallization time for isothermal crystallizations performed at temperatures ranging between 175 ºC and 185 ºC. b) Temperature dependence of the crystal growth rate of spherulites of nylon 12 9. c) Plot of ln $G + U^* / [R (T_c - T_\infty)]$ versus $1 / (T_c \Delta T f)$ to determine the K_g nucleation parameter of nylon 12 9.

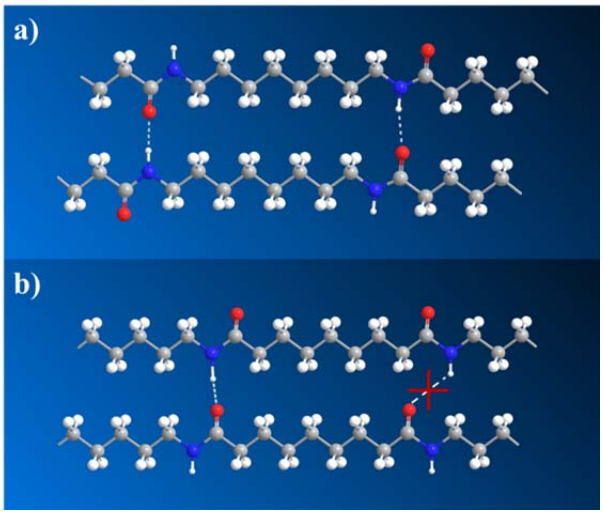

Figure 1

Olmo *et al.*

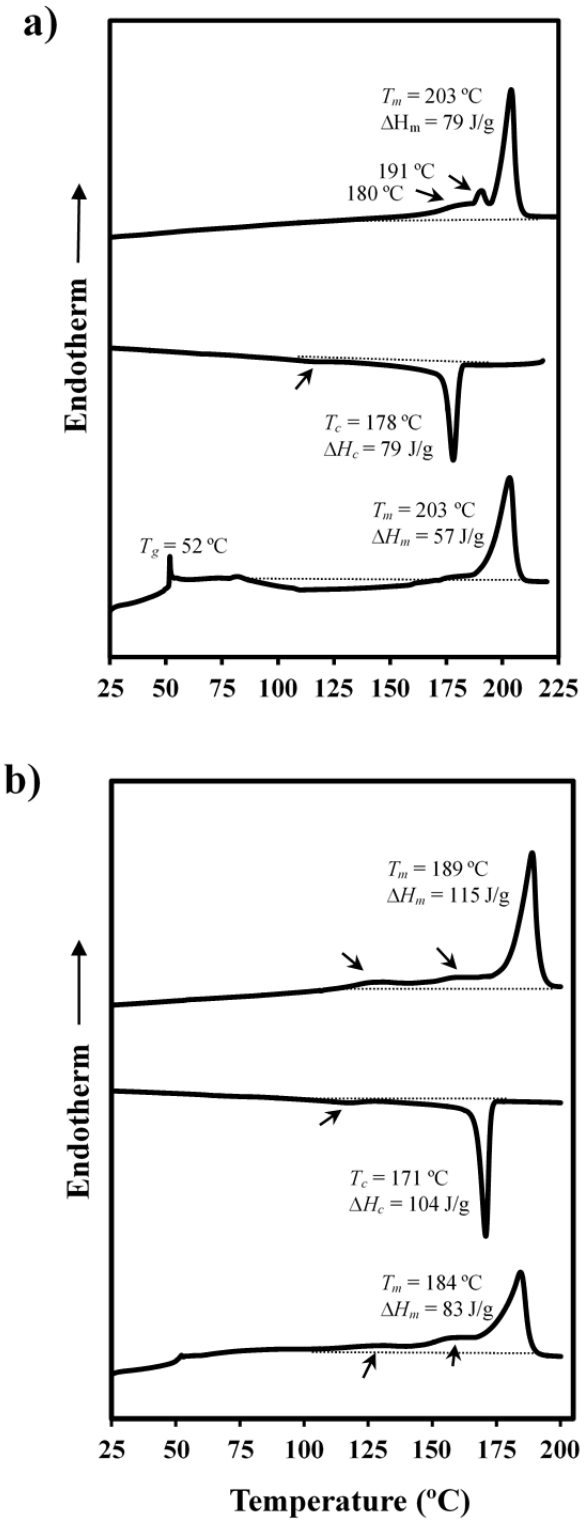

Figure 2

Olmo *et al.*

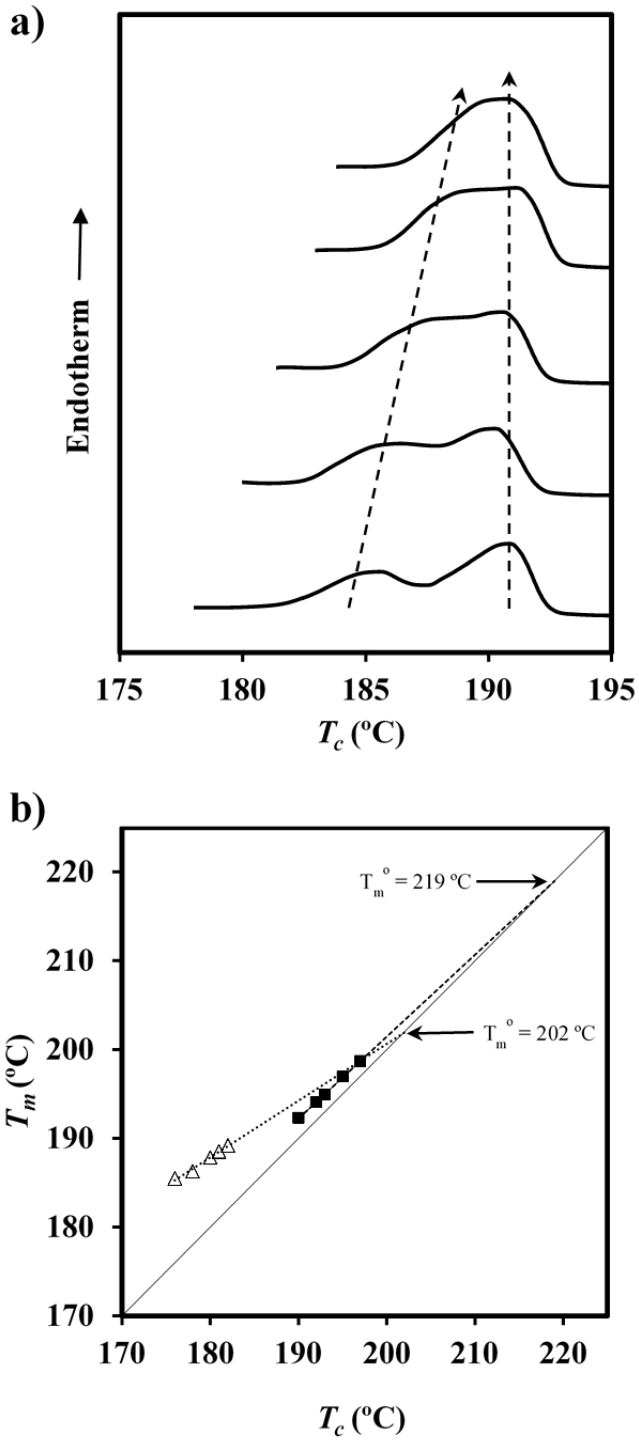

Figure 3

Olmo *et al.*

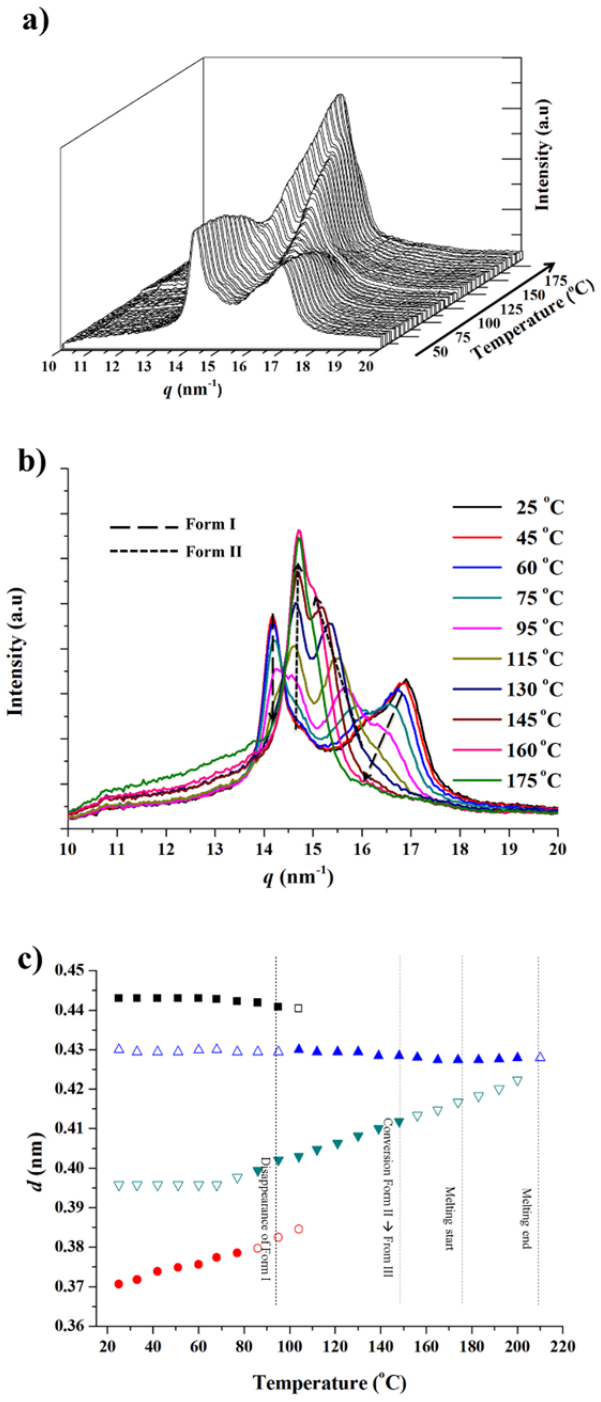

Figure 4

Olmo *et al.*

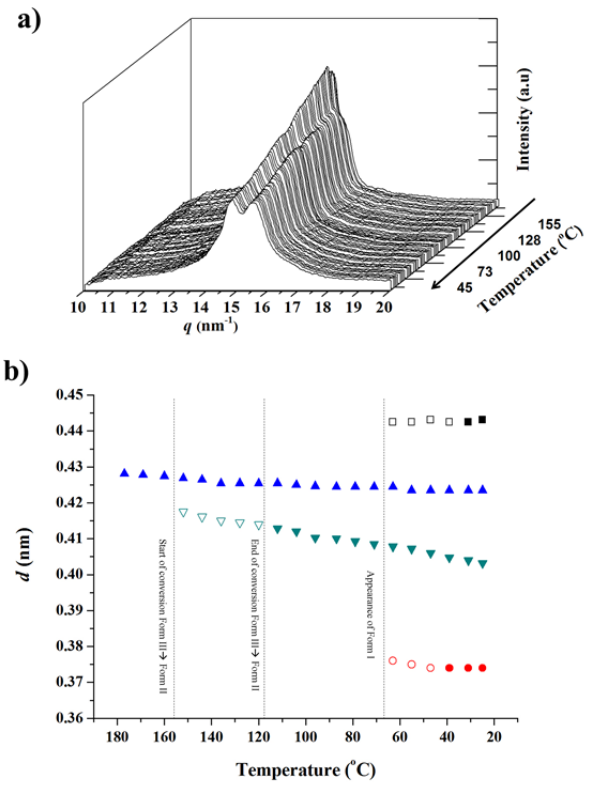

Figure 5

Olmo *et al.*

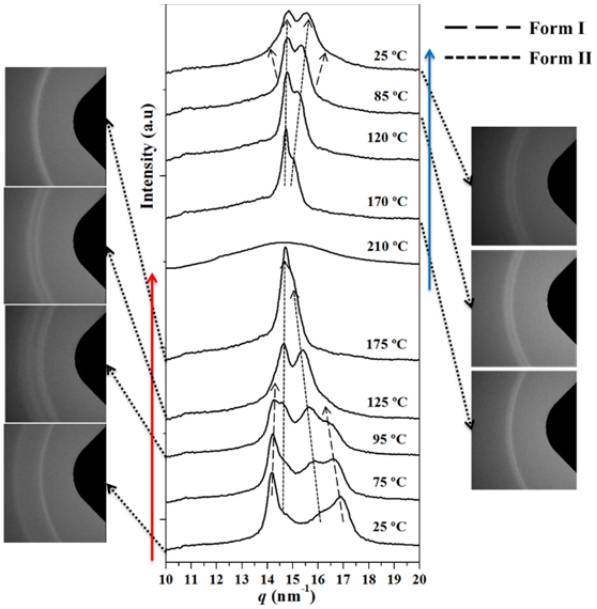

Figure 6

Olmo *et al.*

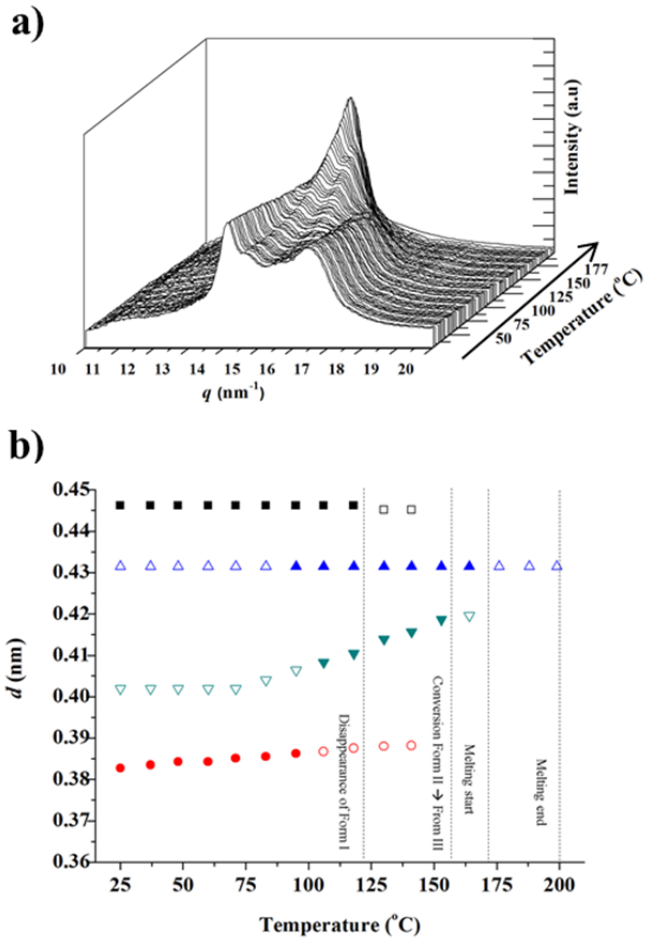

Figure 7

Olmo *et al.*

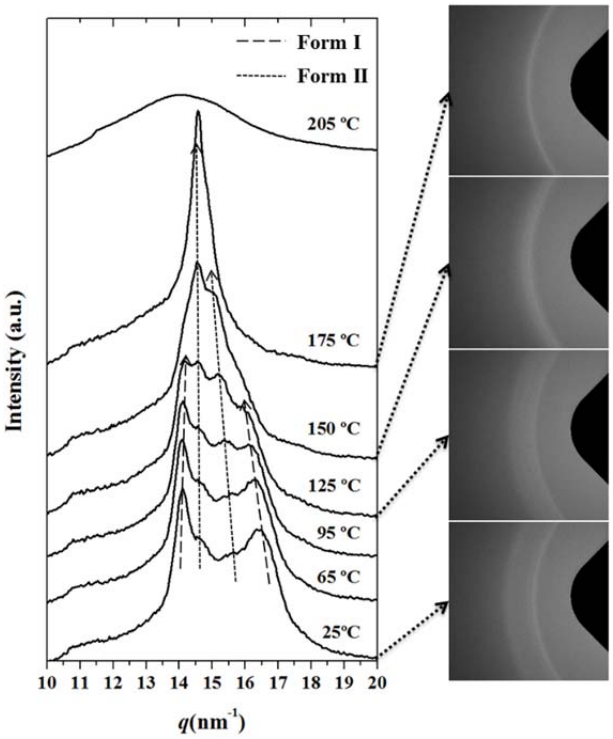

Figure 8

Olmo *et al.*

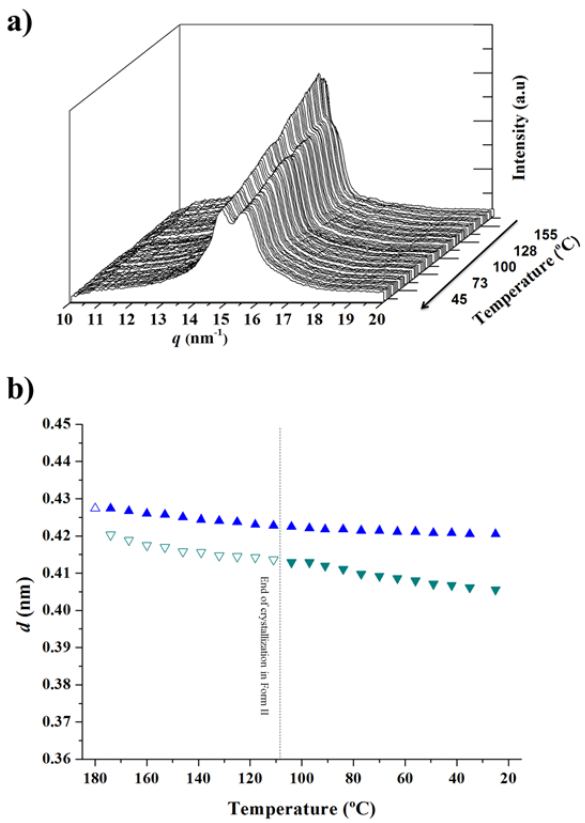

Figure 9

Olmo *et al.*

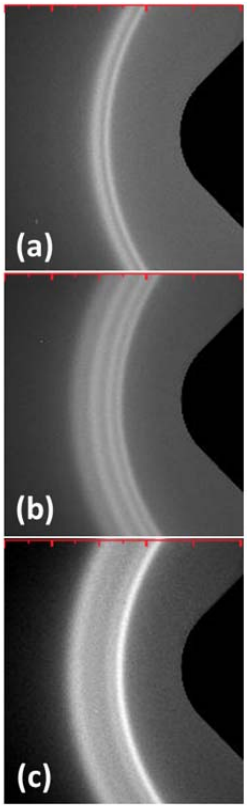

Figure 10
Olmo *et al.*

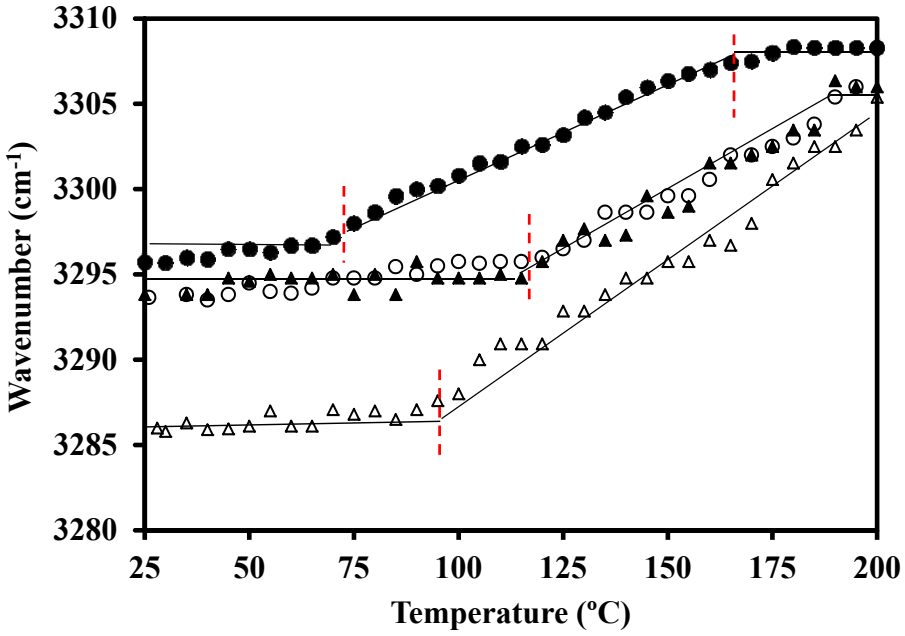

Figure 11
Olmo *et al.*

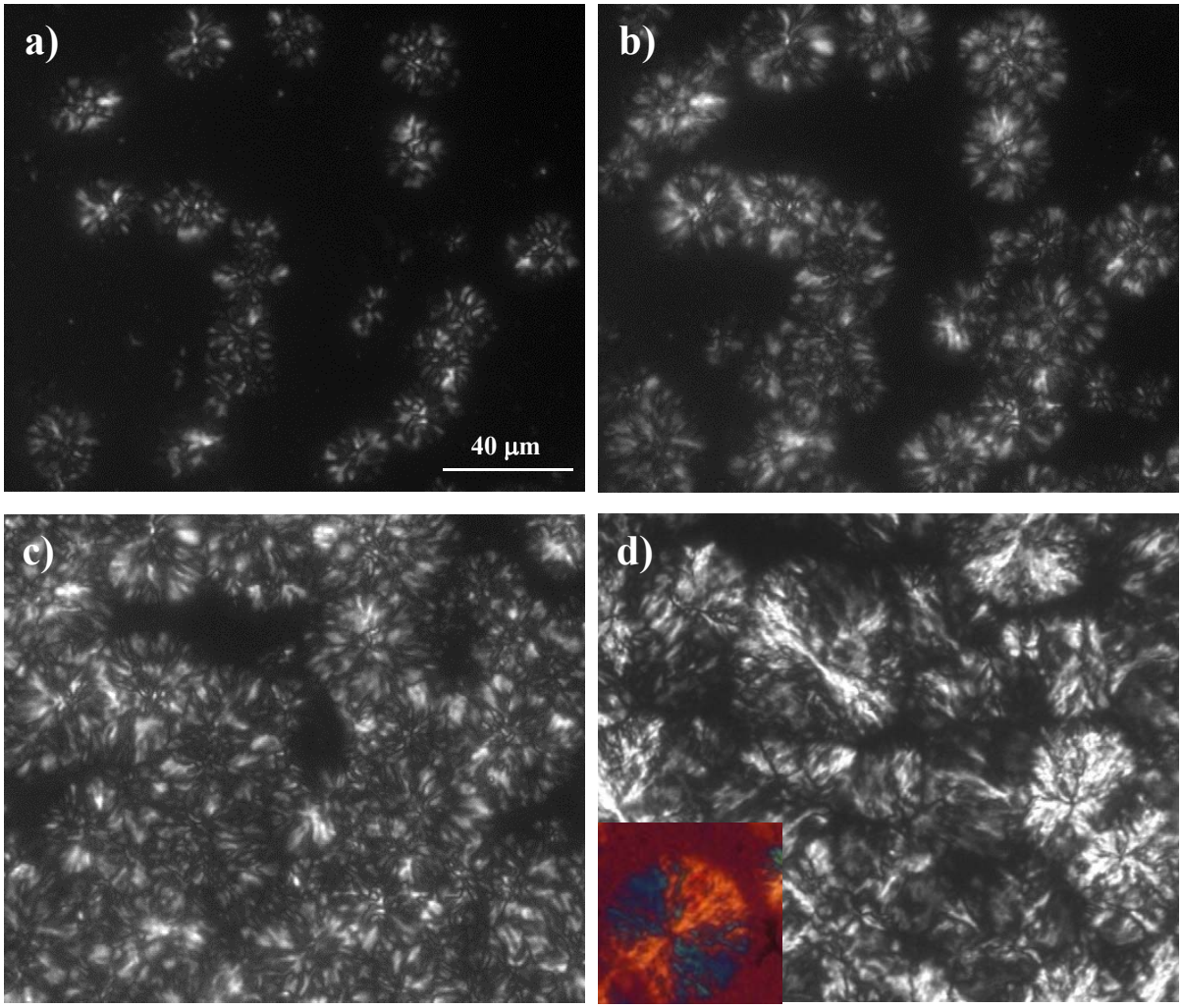

Figure 12

Olmo *et al.*

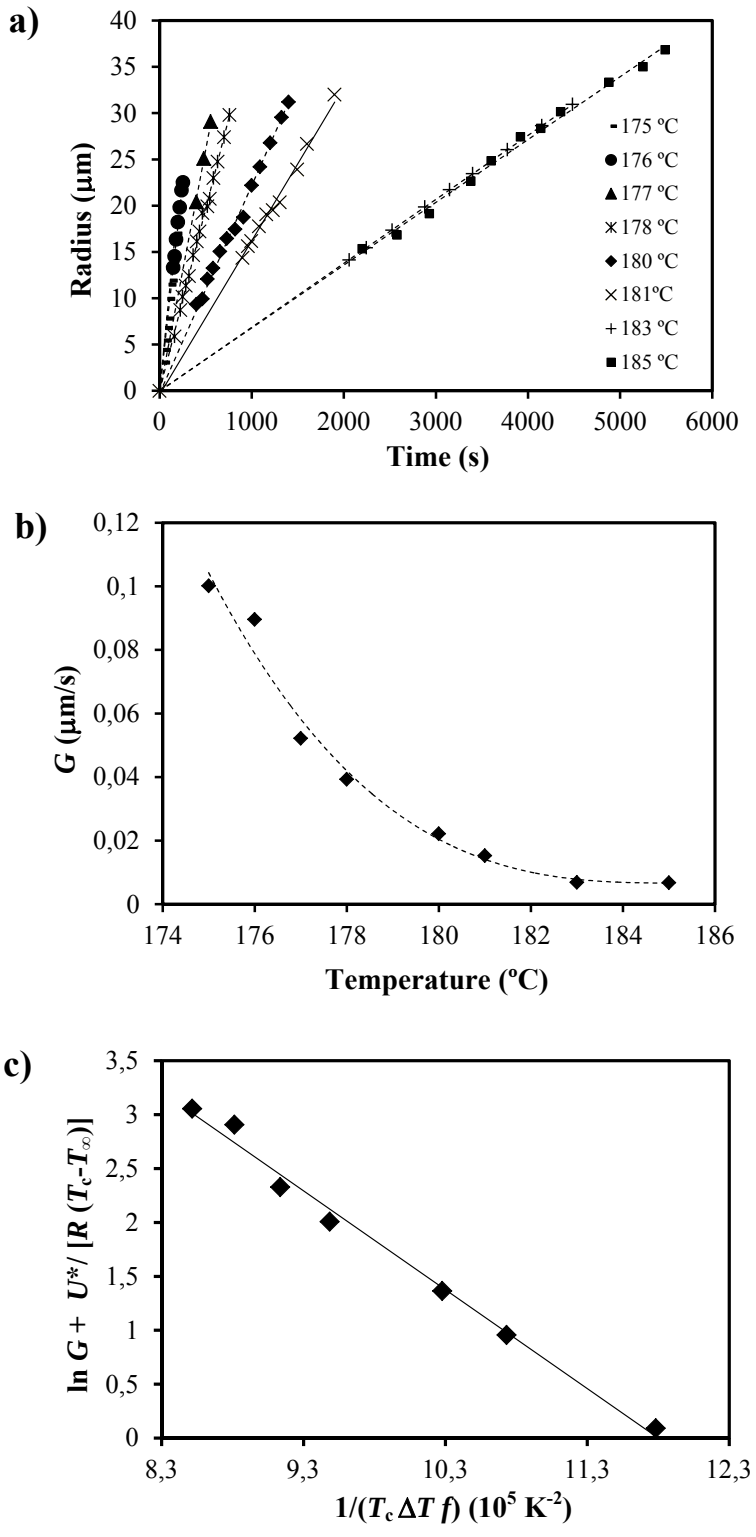

Figure 13
Olmo *et al.*